THE
EMBO
JOURNAL

Lateral assembly of the immunoglobulin protein SynCAM 1 controls its adhesive function and instructs synapse formation

Adam I Fogel[1,3], Massimiliano Stagi[2,3], Karen Perez de Arce[3] and Thomas Biederer*

Department of Molecular Biophysics and Biochemistry, Yale University, New Haven, CT, USA

Synapses are specialized adhesion sites between neurons that are connected by protein complexes spanning the synaptic cleft. These *trans*-synaptic interactions can organize synapse formation, but their macromolecular properties and effects on synaptic morphology remain incompletely understood. Here, we demonstrate that the synaptic cell adhesion molecule SynCAM 1 self-assembles laterally via its extracellular, membrane-proximal immunoglobulin (Ig) domains 2 and 3. This *cis* oligomerization generates SynCAM oligomers with increased adhesive capacity and instructs the interactions of this molecule across the nascent and mature synaptic cleft. In immature neurons, *cis* assembly promotes the adhesive clustering of SynCAM 1 at new axo-dendritic contacts. Interfering with the lateral self-assembly of SynCAM 1 in differentiating neurons strongly impairs its synaptogenic activity. At later stages, the lateral oligomerization of SynCAM 1 restricts synaptic size, indicating that this adhesion molecule contributes to the structural organization of synapses. These results support that lateral interactions assemble SynCAM complexes within the synaptic cleft to promote synapse induction and modulate their structure. These findings provide novel insights into synapse development and the adhesive mechanisms of Ig superfamily members.

Introduction

A defining feature of synaptic ultrastructure is a 'band of material' (Gray, 1959) spanning the even width of the synaptic cleft. This material is organized into periodic strata (Zuber et al, 2005; Rostaing et al, 2006) and consists of protein complexes connecting pre- and post-synaptic membranes (Lucic et al, 2005). These *trans*-synaptic connections likely contribute to the precise alignment of pre- and post-synaptic membrane specializations (Schikorski and Stevens, 1997).

The molecular analysis of the synaptic cleft has identified membrane proteins that can induce synaptic specializations and organize their maturation (Biederer and Stagi, 2008; Jin and Garner, 2008; Giagtzoglou et al, 2009). These proteins include neurexins/neuroligins, EphB receptors, and the SynCAM proteins (synaptic cell adhesion molecules) of the immunoglobulin (Ig) superfamily, also known as nectin-like or Cadm proteins. The homophilic adhesion molecule N-cadherin is additionally present at synapses and regulates their structural and functional maturation (Kwiatkowski et al, 2007; Takeichi, 2007). Preassembly of these adhesion proteins may enable them to contribute to synapse formation, as shown for neuroligin 1 (Dean et al, 2003; Gerrow et al, 2006).

The assembly steps of *trans*-synaptic protein complexes remain insufficiently understood. Even for N-cadherin complexes, the best understood among these adhesion systems, it is debated whether they are formed from lateral *cis* dimers (Troyanovsky et al, 2007; Harrison et al, 2010) or from monomers (Sivasankar et al, 2009; Zhang et al, 2009). Similarly, the contributions of *cis* assembly of Ig proteins to their adhesive interactions remain unclear. This contrasts with the detailed structural views of Ig *trans* dimers that can assemble in a zipper-like manner to form extended structures as shown for NCAM and TAG-1 (Freigang et al, 2000; Soroka et al, 2003), or assemble into separately spaced *trans* dimers through horseshoe-shaped Ig arrangements such as L1 and Dscam (Meijers et al, 2007; He et al, 2009).

To gain molecular insight into the interactions that organize the synaptic cleft, we have analysed the assembly steps of SynCAM 1, the founding member of a family of four Ig superfamily proteins that are most prominently expressed in brain (Biederer, 2006; Thomas et al, 2008). SynCAM proteins contain three extracellular Ig-like domains, one transmembrane region, and a short cytoplasmic tail with protein interaction motifs predicted to bind cytoskeletal regulators and scaffolding molecules. SynCAM 1 is already expressed in neurons prior to synapse formation and its rapid adhesive assembly at axo-dendritic contacts precedes synapse development (Stagi et al, 2010). Subsequently, SynCAM 1 engages in homo- and heterophilic adhesive interactions that induce neurons in the central nervous system to assemble pre- but not post-synaptic specializations (Biederer et al, 2002; Nam and Chen, 2005; Fogel et al, 2007; Robbins et al, 2010). In the peripheral nervous system, SynCAM proteins also mediate interactions of axons with myelinating Schwann cells (Maurel et al, 2007; Spiegel et al, 2007).

Analysing SynCAM adhesion complexes between neurons, we now show that SynCAM 1 is clustered in dendrites of

*Corresponding author. Department of Molecular Biophysics and Biochemistry, Yale University, SHM C127, 333 Cedar Street, New Haven, CT 06520, USA. Tel.: + 1 203 785 5465; Fax: + 1 203 785 6404; E-mail: thomas.biederer@yale.edu
[1]Present address: National Institute of Neurological Disorders and Stroke, NIH, Bethesda, MD 20892, USA
[2]Present address: Department of Neurology, Yale University, New Haven, CT 06520, USA
[3]These authors contributed equally to this work

developing neurons prior to synaptic contact. We find that the extracellular Ig-like domains 2 and 3 of SynCAM 1 can self-assemble independently of adhesive extracellular interactions or intracellular scaffolds. Notably, these *cis* interactions of SynCAM 1 promote its adhesive *trans* binding in heterologous cells and at axo-dendritic contacts between immature neurons. In addition, lateral SynCAM 1 interactions increase its ability to recruit cognate SynCAM binding partners across the nascent synaptic cleft and to induce pre-synaptic specializations. At mature post-synaptic sites, the *cis* oligomerization of SynCAM 1 then contributes to restricting the size of synaptic specializations. These results identify the lateral self-assembly of the Ig protein SynCAM 1 as a novel determinant in the *trans*-synaptic organization of developing and mature synapses.

Results

SynCAM 1 assembles into stable clusters in the absence of adhesive contacts

To determine the distribution of SynCAM in neuronal membranes prior to synaptogenesis, we stained surface-expressed SynCAM 1 in live hippocampal neurons at 5 days *in vitro* (d.i.v.) using antibodies against an extracellular epitope. Neuronal cell bodies and dendrites were labelled using antibodies against MAP2 (microtubule-associated protein 2). We

found that endogenous SynCAM 1 protein appeared in clusters on MAP2-positive dendrites (Figure 1A, left). SynCAM 1 signal was absent in hippocampal cultures from SynCAM 1 knockout mice (Figure 1A, right). We next addressed the mobility of these SynCAM 1 clusters by imaging a SynCAM 1 construct carrying an extracellular insertion of the pH-sensitive GFP variant pHluorin. This construct allows to selectively visualize the surface pool of this membrane protein (Stagi *et al*, 2010). SynCAM 1-pHluorin was clustered on the neurites, similar to the endogenous protein, and these packets were mostly immobile (Figure 1B).

To gain biochemical insight into SynCAM 1 clustering, we treated SynCAM 1-expressing COS7 cells with the membrane impermeable, 11 Å long cross-linker bis-sulfosuccinimidyl suberate (BS^3). Cells were physically separated during cross-linking to prevent adhesive interactions. As shown by immunoblotting of cell lysates, surface SynCAM 1 molecules of these isolated cells were efficiently cross-linked into higher molecular weight species that likely correspond to dimers and larger oligomers (Figure 1C). These findings extend a previous report that SynCAM 1 forms homodimers upon heterologous expression (Masuda *et al*, 2002) and indicate that a significant fraction of SynCAM 1 assembles into higher oligomeric species in the plasma membrane of neurons and non-neuronal cells.
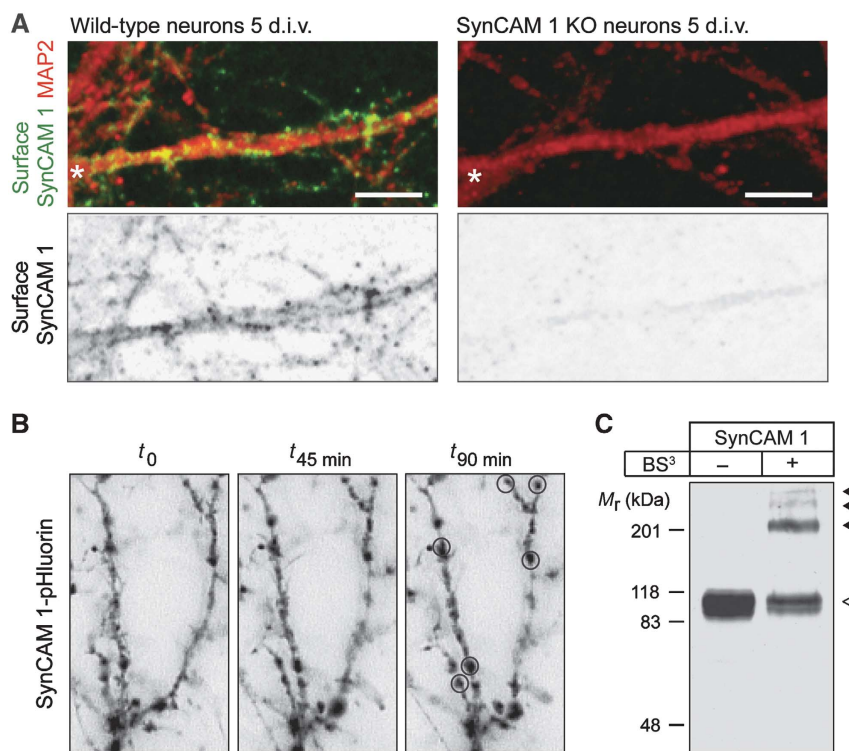

Figure 1 SynCAM 1 assembles into discrete clusters in the absence of adhesive contact. (**A**) SynCAM 1 forms dendritic clusters prior to the onset of synaptogenesis. Dissociated hippocampal wild-type mouse neurons (left) were labelled live at 5 d.i.v. with antibodies against an extracellular SynCAM 1 epitope (green) and then stained for the dendritic marker MAP2 (red). Parallel analysis of neurons from SynCAM 1 knockout (KO) littermate mice demonstrates antibody specificity (right). Neurites decorated with anti-SynCAM 1 antibodies correspond to dendrites based on their MAP2 signal, thickness and length, and did not contact other neurons. Top panels, merged images. Bottom, SynCAM 1 signals. Asterisks mark cell bodies. Scale bar, 5 μm. (**B**) SynCAM 1 assemblies are stable on neurite surfaces. Hippocampal neurons expressing pHluorin-tagged SynCAM 1, which selectively visualizes its surface population, were imaged live at 5 d.i.v. on a spinning disc microscope. Most surface clusters of SynCAM 1-pHluorin were immobile over the 90-min recording period, with examples marked by circles in the last frame. (**C**) SynCAM 1 oligomerizes *in cis*. Physically isolated COS7 cells expressing full-length SynCAM 1 were incubated in the absence (lane 1) or presence (lane 2) of the membrane impermeable cross-linker BS^3. SynCAM 1 was detected by immunoblotting at its apparent molecular weight of 100 kDa in controls (left lane; open arrowhead). Cross-linking converted it into higher molecular weight species (right lane; filled arrowheads).

SynCAM 1 extracellular sequences are in close contact

To characterize the interactions underlying lateral SynCAM 1 assembly, we performed Förster resonance energy transfer (FRET) analyses of Cherry- and pHluorin-tagged SynCAM 1 proteins (Figure 2A). FRET between this acceptor and donor pair was measured in live COS7 cells using acceptor photobleaching. The use of pHluorin ensured that only FRET between surface-expressed SynCAM 1 proteins was detected. Efficient FRET was measured between SynCAM 1-Cherry and SynCAM 1-pHluorin (Figure 2B and C; Supplementary Table S1). This demonstrates the close proximity of SynCAM 1 monomers in these clusters, as FRET typically occurs over distances shorter than 10 nm (Wouters *et al*, 2001). Cells co-expressing soluble Cherry and GFP served as negative control for FRET (Supplementary Figure S1; Supplementary Table S1). Additional controls confirmed that FRET of live and fixed samples yielded identical measurements, and that neither donor bleaching nor bleed-through of excitation light occurred (data not shown). Adhesive interactions between

SynCAM 1-Cherry and SynCAM 1-pHluorin expressed individually in cells contacting each other did not result in a FRET signal (Supplementary Figure S2A and B; Supplementary Table S1). This indicates that the Ig domains of SynCAM 1 assemble into anti-parallel *trans* complexes, consistent with their crystallographic analysis (Fogel *et al*, 2010), rather than forming parallel zippers along their extracellular sequences (Supplementary Figure S2C). Together, these results show that SynCAM 1 molecules efficiently oligomerize *in cis*.

The Ig-like domains 2 and 3 drive cis assembly of SynCAM 1

Are SynCAM 1 molecules clustered by intracellular scaffolds or through lateral extracellular interactions? To determine whether the extracellular sequence of SynCAM 1 is sufficient for clustering, we developed an extracellular domain ECD[flag]–GPI construct comprised of the three SynCAM 1 Ig domains in which the transmembrane and intracellular sequences were replaced by a GPI anchor. A flag epitope was inserted between
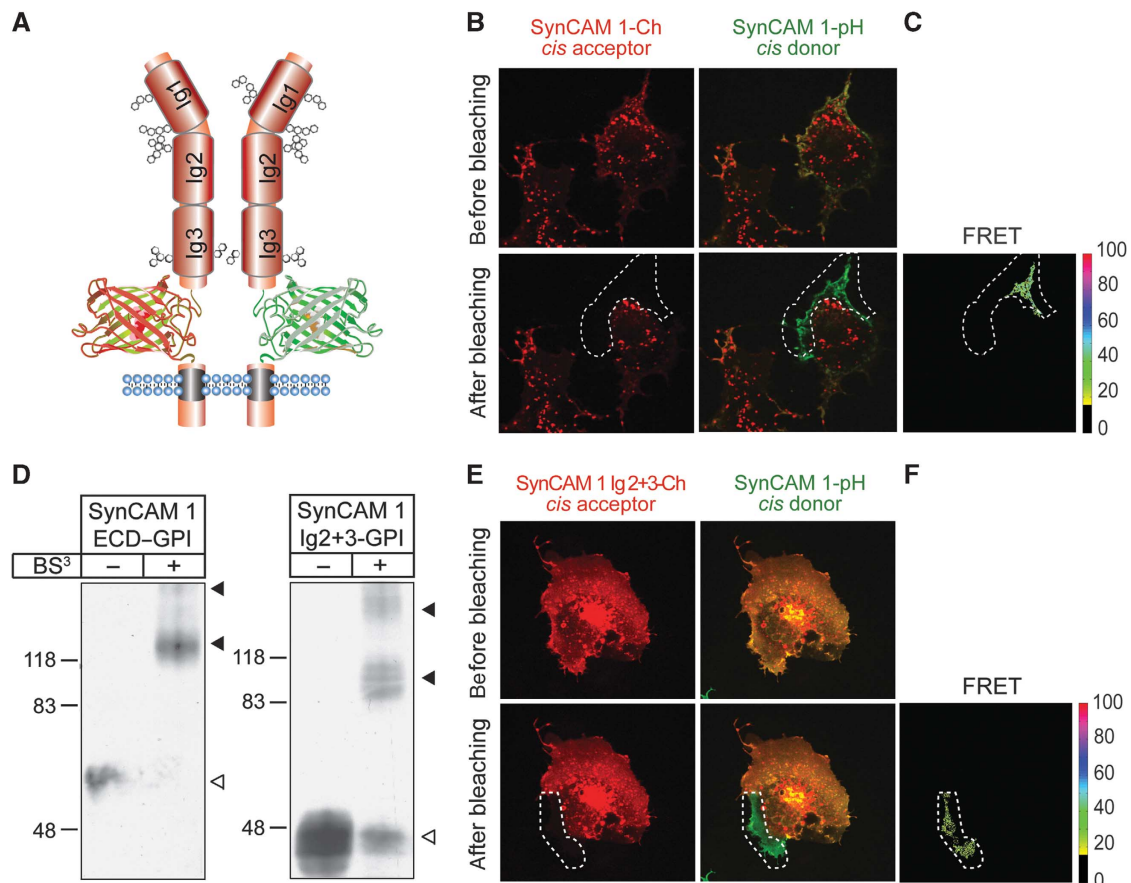

Figure 2 SynCAM 1 oligomerization in membranes is mediated by domains Ig2 and Ig3. (**A**) Model of the Cherry- and pHluorin- tagged SynCAM 1 constructs used as FRET acceptor and donor pair, respectively. Hexagons indicate N-linked glycans. (**B**) SynCAM 1-Cherry (Ch) and SynCAM 1-pHluorin (pH) were co-expressed in COS7 cells and FRET was analysed by acceptor photobleaching. Top row, Cherry acceptor signal (left column) and merged image with the pHluorin donor signal (right) before bleaching. Bottom, signals immediately after bleaching of Cherry in the marked area. The increase in SynCAM 1-pH signal after bleaching the SynCAM 1-Ch donor demonstrates FRET. (**C**) FRET signal measured in (**B**), depicted on a pseudocolour scale. The fraction of pixels in which FRET was measured after photobleaching was $29.3 \pm 9.9\%$ ($n = 6$ cells). (**D**) Ig domains $2 + 3$ mediate SynCAM 1 *cis* oligomerization. Constructs encoding the full extracellular domain of SynCAM 1 (ECD; left panel) or the Ig2 + 3 domains (right) followed by a flag epitope and a GPI anchor were expressed in COS7 cells. Cells were incubated in the absence or presence of the cross-linker BS[3] as indicated. Cells were suspended during cross-linking to prevent adhesive *trans* interactions. SynCAM ECD[flag] and Ig2 + 3[flag]-GPI were detected by anti-flag immunoblotting at 65 and 45 kDa, respectively, in controls (open arrowheads) and were cross-linked to a similar extent into higher molecular weight oligomers (filled arrowheads). (**E**) Cherry-tagged SynCAM 1 Ig2 + 3 and full-length SynCAM 1-pHluorin were co-expressed in COS7 cells. FRET was detected by acceptor photobleaching as in (**B**). (**F**) FRET signal measured in (**E**), depicted on a pseudocolour scale. The fraction of pixels showing FRET after photobleaching was $14.0 \pm 5.9\%$ ($n = 6$ cells), demonstrating lateral interactions of the Ig2 + 3 protein with full-length SynCAM 1.

the ECD and the GPI anchor, facing the extracellular space, and live labelling with anti-flag antibodies confirmed that ECD[flag]–GPI was tethered to the cell surface in COS7 cells (see below, Figure 4A, and Supplementary Figure S3). Cross-linking demonstrated that ECD[flag]–GPI forms oligomers (Figure 2D, left panel), similar to full-length SynCAM 1 (Figure 1C).

As the first Ig-like domain of SynCAM 1 is required and sufficient for adhesive *trans* binding (Fogel *et al*, 2010), we hypothesized that the other two Ig-like domains may mediate the *cis* interactions we observed. To test this, we generated a flag-tagged, GPI-anchored construct of both Ig2 and Ig3 domains, which sorts to the plasma membrane as expected (see Figure 4A). This Ig2 + 3[flag]-GPI protein was cross-linked into oligomers to a similar extent as the full-length SynCAM 1 extracellular sequence, showing that these domains interact *in cis* (Figure 2D, right panel).

If the Ig domains 2 + 3 are sufficient to cluster SynCAM 1, their co-expression with wild-type SynCAM 1 should result in mixed clusters on the cell surface. To address this, we measured FRET in COS7 cells co-expressing full-length SynCAM 1-pHluorin with SynCAM 1 Ig2 + 3-Cherry. FRET was readily detected between both proteins, confirming the formation of mixed surface clusters (Figure 2E and F; Supplementary Table S1). Together, these results demonstrate that the Ig domains 2 + 3 of SynCAM 1 are sufficient to drive the lateral assembly of SynCAM 1 monomers.

SynCAM 1 clusters are maintained by cis interactions of Ig2 + 3 in neurons

As the Ig2 + 3 domains can laterally assemble SynCAM 1, we asked whether these interactions are required to maintain SynCAM 1 clusters in developing neurons. Clusters were

visualized by imaging SynCAM 1-pHluorin in dissociated rat hippocampal neurons. Cultures were treated at 6 d.i.v. for 2 h either with IgG protein as control or with a soluble fusion protein of the Ig domains 2 + 3 with IgG1-F$_c$ purified from heterologously expressing cells. IgG-treated control cells showed, as expected, SynCAM 1-pHluorin clusters on MAP2-positive dendrites (Figure 3A, left panels). On the other hand, exogenous addition of the Ig2 + 3 fusion protein to live neurons acutely reduced SynCAM 1-pHluorin cluster density by $48 \pm 4\%$ ($P < 0.0001$) and area by $25 \pm 7\%$ ($P = 0.027$) (Figure 3A, right panels and B). This is consistent with a requirement for Ig2 + 3 interactions in maintaining lateral assemblies of SynCAM 1 in neuronal membranes.

Cis assembly of SynCAM 1 promotes trans adhesion strength

To address whether the self-assembly of SynCAM 1 contributes to its adhesive interactions, we employed a cell overlay approach. As positive control, we expressed the ECD[flag]–GPI construct of SynCAM 1 in COS7 cells and overlaid the live cells with the purified, soluble extracellular SynCAM 2 sequence fused to IgG1-F$_c$ (Figure 4A, left column) (Thomas *et al*, 2008). For each analysed cell, the amount of surface-expressed ECD[flag]–GPI was measured by fluorescence microscopy after the addition of primary anti-flag and fluorophore-labelled secondary antibodies to live cells, while the retained SynCAM 2 ECD-F$_c$ was detected using fluorescent Protein A. SynCAM 1 Ig2 + 3-GPI served as negative control for SynCAM 2 retention (right column), as it lacks the Ig1 domain required for *trans* binding (Fogel *et al*, 2010).

If the self-assembly of SynCAM 1 is important for its adhesive interaction, the formation of mixed *cis* clusters
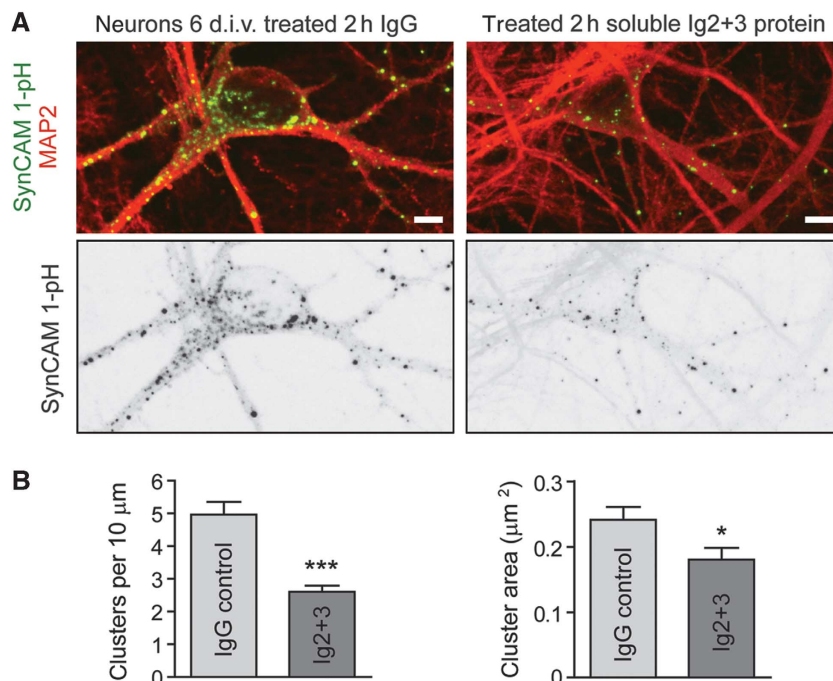

Figure 3 Lateral interactions are required to maintain SynCAM 1 clusters in neurons. (**A**) Dissociated hippocampal neurons expressing SynCAM 1-pHluorin (green) were treated at 6 d.i.v. for 2 h with IgG control protein (left panels) or a purified, soluble SynCAM 1 Ig2 + 3 fusion protein (right). Cells were then fixed and stained for the dendritic marker MAP2 (red). Top panels, merged images. Bottom, SynCAM 1 signal. Scale bar, 5 μm. (**B**) Quantification of results in (**A**). Acute addition of the Ig2 + 3 domains reduced SynCAM 1-pHluorin cluster density and area (IgG, $n = 21$ dendritic segments from 17 neurons; Ig2 + 3, $n = 20$ dendritic segments from 13 neurons; two independent experiments). *$P < 0.05$; ***$P < 0.001$.
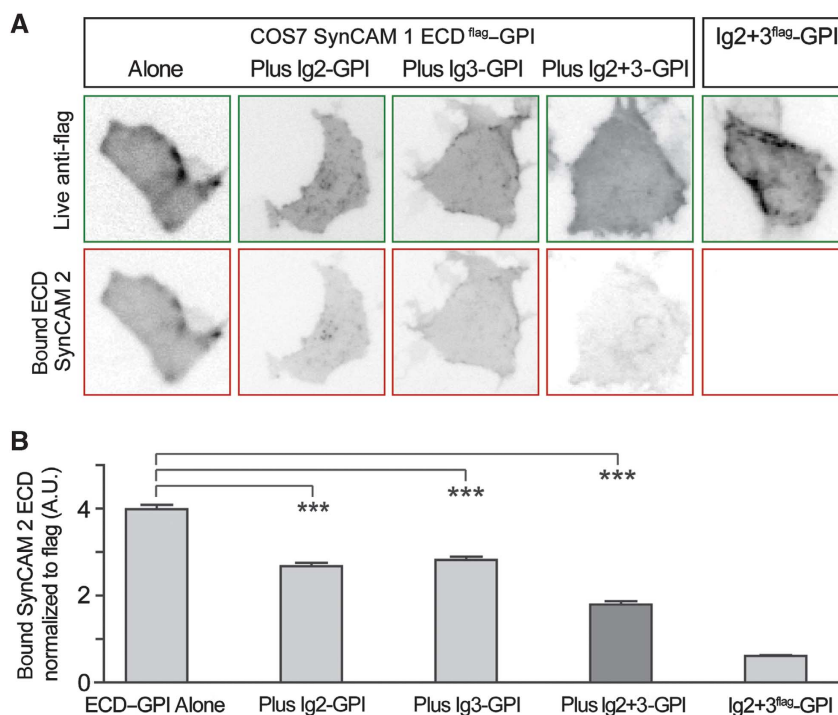
Figure 4 *Cis* assembly of SynCAM 1 strengthens *trans* adhesion. (**A**) The SynCAM 1 Ig2 + 3 domains act *in cis* to reduce adhesive *trans* binding of SynCAM 1. COS7 cells expressed SynCAM 1 ECD[flag]–GPI either alone (left column) or co-expressed the indicated GPI-anchored Ig domains lacking a flag epitope. Surface-expressed ECD[flag]–GPI was labelled live with anti-flag and secondary fluorescent antibodies (top row, green). Cells were simultaneously overlaid with the soluble SynCAM 2 ECD fused to IgG1-F_c, which was visualized with fluorophore-labelled protein A (bottom, red). The non-adhesive Ig2 + 3[flag]-GPI served as negative control for SynCAM 2 retention (right column). (**B**) Quantification of results in (**A**). *Y* axis, fluorescence signal of bound SynCAM 2 ECD normalized to the flag signal of cell-expressed SynCAM 1 ECD[flag]–GPI. Co-expression of the Ig2 or Ig3 domain reduced the adhesive retention of the SynCAM 2 ECD by SynCAM 1, while the Ig2 + 3 construct inhibited even more strongly (ECD, $n = 147$ cells; plus Ig2, $n = 192$; plus Ig3, $n = 195$; plus Ig2 + 3, $n = 169$; Ig2 + 3 alone, $n = 220$). ***$P < 0.001$.

between its full extracellular sequence and individual Ig domains should reduce the adhesion competence of the full-length SynCAM 1 protein. We tested this using the GPI-anchored Ig2 and Ig3 domains, which do not mediate *trans* adhesion (Fogel *et al*, 2010). Our results show that Ig2-GPI or Ig3-GPI reduced the ability of co-expressed ECD[flag]–GPI to retain overlaid SynCAM 2 by 33 ± 3 and $29 \pm 3\%$, respectively (Figure 4B). Co-expression of an Ig2 + 3-GPI construct reduced the interaction of ECD[flag]–GPI with overlaid SynCAM 2 even more by $55 \pm 3\%$. All SynCAM constructs were expressed equally well and their co-expression did not alter the surface expression of ECD[flag]–GPI (Supplementary Figure S3 and data not shown). The formation of SynCAM 1 *cis* oligomers through the Ig2 + 3 domains therefore contributes importantly to its adhesive strength. This demonstrates that the lateral self-assembly of this Ig protein can modulate its *trans* interactions.

Axo-dendritic contact assembly of SynCAM 1 involves *cis* interactions

The first known developmental role of SynCAM 1 in neuronal adhesion is to rapidly cluster at axo-dendritic contact sites, indicative of functions of this protein in sensing growth cone contact (Stagi *et al*, 2010). We tested whether the *cis* assembly of SynCAM 1 contributes to the dynamic formation of these contacts. Growth cones marked by SynCAM 1-pHluorin were imaged live at 5 d.i.v. as they migrated towards neurites also expressing this fusion protein. Contact resulted in a rapid 1.9 ± 0.07-fold increase in pHluorin fluorescence intensity in the contact area (Figure 5A and C) as described previously

(Stagi *et al*, 2010). This contact-induced clustering requires the SynCAM 1 Ig1 domain that is also necessary for SynCAM 1-mediated cell adhesion (Stagi *et al*, 2010), indicating that the fluorescence increase corresponds to the adhesive assembly of SynCAM 1 upon axo-dendritic surface interactions. We next analysed contacts of growth cones with neurites that both co-expressed SynCAM 1-pH and the Ig2 + 3-GPI construct. Notably, interfering with the lateral Ig2 + 3 interactions of SynCAM 1 reduced its contact-induced clustering to 1.4 ± 0.04-fold (Figure 5B and C). Ig2 + 3-GPI did not alter the previously described activity of SynCAM 1 to down-regulate the number of growth cone filopodia (Stagi *et al*, 2010) (control, 4.7 ± 1.7 filopodia per growth cone; SynCAM 1-pH, 1.7 ± 1.3; SynCAM 1-pH plus Ig2 + 3-GPI, 1.2 ± 1.1; $n = 4$ growth cones each). This lack of an effect on filopodia number supports that Ig2 + 3-GPI expression specifically interferes with adhesive SynCAM functions. These results demonstrate that the *cis* interactions of SynCAM 1 in neuronal plasma membranes promote its local clustering when growth cones and neurites contact each other.

SynCAM 1 *cis* assembly promotes the adhesive recruitment of SynCAMs in synapse induction

We next tested the functions of lateral SynCAM 1 interactions for its synapse-organizing activity, and co-cultured non-neuronal cells that heterologously expressed SynCAM 1 constructs with dissociated neurons (Biederer and Scheiffele, 2007). GFP marked transfected COS7 cells. Expression of the full SynCAM 1 ECD–GPI in co-cultured COS7 cells was
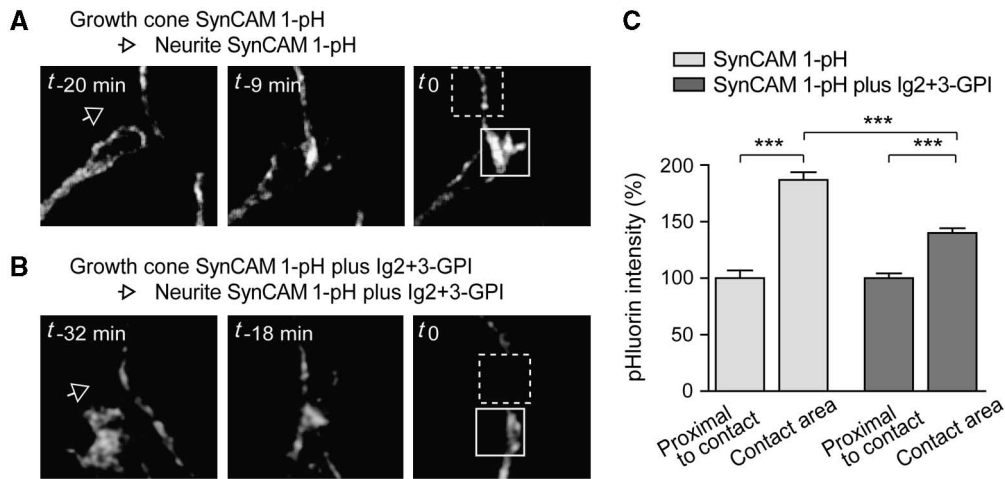
Figure 5 *Cis* interactions of SynCAM 1 promote its clustering at growth cone contacts. (**A**) Growth cones of dissociated hippocampal neurons expressing SynCAM 1-pHluorin (pH) were imaged at 5 d.i.v. as they advanced towards neurites that also expressed SynCAM 1-pH. The arrowhead marks the growth cone direction. Boxes indicate the contact area (solid line) and a proximal area of the neurite (dashed line). t_0 is the time point of stable contact formation. (**B**) Neurons co-expressing SynCAM 1-pH with GPI-anchored SynCAM 1 Ig2 + 3 were imaged as in (**A**). Note that the shown growth cone aligned itself with the neurite once a stable contact was formed. (**C**) Quantification of SynCAM 1-pH clustering at growth cone contacts. Fluorescence intensity was measured in growth cone areas contacting a neurite and from the proximal, non-contacted areas. Imaging was performed as in (**A**, **B**) and quantification shows that SynCAM 1 accumulation at growth cone contact areas involves *cis* interactions (SynCAM 1-pH alone, $n = 5$ contacts; SynCAM 1-pH plus Ig2 + 3, $n = 7$). ***$P < 0.001$.

sufficient to recruit neuronal SynCAM proteins to contact sites (Figure 6A, left column). This was determined by staining co-cultures with antibodies detecting the SynCAM carboxyl-terminal tail, which only recognize neuronal full-length SynCAMs but not the COS7-cell expressed GPI-anchored constructs that lack this tail. Notably, the co-expression of the GPI-anchored Ig2 + 3 domains with ECD–GPI in COS7 cells reduced the recruitment of neuronal SynCAMs to neuron-COS7 cell contacts by $55 \pm 10\%$ (Figure 6A and B). As expected, the non-adhesive Ig2 + 3-GPI construct did not recruit neuronal SynCAMs, similar to negative control cells expressing GFP alone.

These experiments were additionally analysed for the ability of COS7-cell expressed SynCAM 1 to induce neuronal specializations containing the pre-synaptic marker SV2 (Figure 6A). Expression of the SynCAM 1 ECD–GPI in COS7 cells resulted in the accumulation of neuronal SV2 proteins atop contacted COS7 cells (ECD, 1.60 ± 0.21 arbitrary fluorescence units; GFP, 1.0 ± 0.20 AFU; $P = 0.008$; for n of cells, see legend of Figure 6B), as shown previously for full-length SynCAM 1 (Biederer *et al*, 2002; Fogel *et al*, 2007). Notably, co-expression of Ig2 + 3-GPI with ECD–GPI in the same COS7 cell abolished the activity of the full extracellular sequence to recruit SV2 (ECD plus Ig2 + 3, 1.2 ± 0.15 A.U.). The Ig2 + 3-GPI construct that lacks adhesive binding and did not recruit neuronal SynCAMs (see above) did not induce SV2 clustering as expected (1.02 ± 0.16 AFU).

We next tested whether the Ig2 + 3 protein can attenuate the induction of pre-synaptic assembly by SynCAM 1 when added exogenously to the co-cultures, that is, independent of co-overexpression with the SynCAM 1 ECD. Using the mixed co-culture approach, HEK293 cells expressing SynCAM 1 were co-cultured in the presence of either control IgG protein or the purified, soluble Ig2 + 3 protein and stained for the pre-synaptic active zone marker bassoon (Figure 6C). Negative control cells expressed only the transfection marker CFP. The results show that the exogenous addition of soluble Ig2 + 3

abrogates the activity of full-length SynCAM 1 to induce pre-synaptic sites (Figure 6D). This is consistent with the Ig2 + 3 protein interfering with lateral interactions of SynCAM in neurons, co-cultured HEK293 cells or both to reduce *trans*-synaptic interactions. The assembly of SynCAM 1 *in cis* therefore likely contributes to the adhesive recruitment of neuronal SynCAMs across synaptic contacts and to the induction of synapses.

SynCAM 1 self-assembly contributes to the structural properties of synaptic specializations

SynCAM 1 is not only present at developing synapses but is also a component of mature synaptic sites (Robbins *et al*, 2010). To determine whether SynCAM 1 self-assembly *in cis* alters the structural organization of synapses, we expressed either soluble Cherry alone or co-expressed Cherry and SynCAM 1 Ig2 + 3-GPI in cultured hippocampal neurons. This construct did not alter the apparent complexity or thickness of dendrites (data not shown), and Ig2 + 3-GPI was present at the synaptic sites of mature neurons, presumably due to lateral interactions with endogenous SynCAM 1 (Supplementary Figure S4). To analyse synaptic structure, neuronal cultures expressing Ig2 + 3-GPI were immunostained at 21 d.i.v. for the post-synaptic marker Shank (Figure 7A). Shank puncta density along the dendrites of these mature neurons was unaltered (data not shown), presumably due to redundant roles of other synapse-organizing proteins in the formation and maintenance of synapses between neurons. However, morphometric analysis revealed a $59 \pm 19\%$ increase in average Shank puncta area upon dendritic expression of Ig2 + 3-GPI compared with control neurons ($P = 0.008$). This was due to area increases in the majority of Shank puncta (Figure 7B). We next addressed whether the post-synaptic expression of Ig2 + 3-GPI also acts across the synaptic cleft to alter pre-synaptic morphological properties and analysed the vesicle marker SV2 (Figure 7C). As with Shank, SV2 puncta density was unaltered (data not
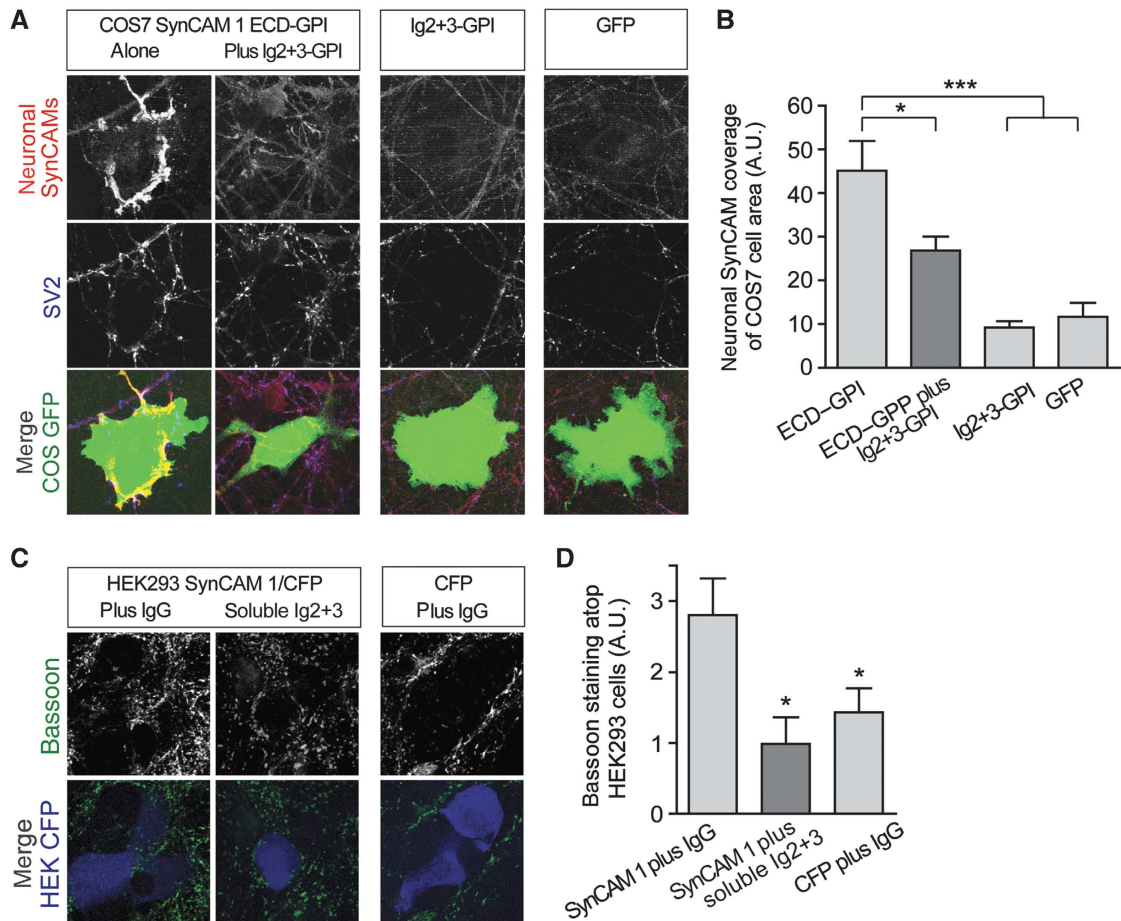
Figure 6 *Cis* oligomerization of SynCAM 1 strengthens *trans*-synaptic interactions and synapse induction. (**A**) Interference with lateral SynCAM 1 assembly *in cis* reduces its ability to recruit neuronal SynCAMs and induce pre-synaptic specializations. The GPI-anchored full SynCAM 1 ECD was expressed in COS7 cells either alone or with the Ig2 + 3-GPI construct. GFP was co-transfected to identify transfected cells. Cells were co-cultured with dissociated hippocampal neurons and immunostained 2 days later for neuronal SynCAM proteins and the pre-synaptic marker SV2. Note that the intracellular epitope used to detect neuronal SynCAM proteins is absent from GPI-anchored constructs. The GPI-anchored SynCAM 1 ECD expressed in COS7 cells recruited neuronal SynCAM proteins and SV2 to contact sites with neurites (first column). This interaction was inhibited by co-expression of Ig2 + 3-GPI in COS7 cells (second column). COS7 cells expressing GPI-anchored SynCAM 1 Ig2 + 3 or GFP alone served as negative control (third and fourth column). (**B**) Quantification of results in (**A**). The bar graphs show the fluorescence intensity of neuronal SynCAMs recruited to COS7 cells expressing the indicated constructs, normalized to the surface area of analysed COS7 cells (ECD–GPI, $n = 33$ cells; ECD–GPI plus Ig2 + 3, $n = 35$; Ig2 + 3, $n = 39$; GFP, $n = 37$; three independent experiments). (**C**) Exogenous interference with lateral SynCAM 1 interactions abrogates its synaptogenic activity. HEK293 cells expressing full-length SynCAM 1 were co-cultured with hippocampal neurons in the presence of control IgG protein (first column) or purified, soluble Ig2 + 3 protein (second column), and were immunostained 2 days later for the pre-synaptic marker bassoon (green). CFP (blue) marked transfected cells. HEK293 cells expressing CFP alone and co-cultured in the presence of IgG served as negative control (third column). (**D**) Quantification of results in (**C**). Addition of the Ig2 + 3 protein prevented the activity of SynCAM 1 to induce bassoon-positive pre-synaptic specializations (SynCAM 1 plus IgG, $n = 13$ cells; SynCAM 1 plus Ig2 + 3, $n = 8$; CFP plus IgG, $n = 14$; two independent experiments). *$P < 0.05$; ***$P < 0.001$.

shown), but quantitative analysis demonstrated a $21 \pm 8\%$ increase in the area of SV2 puncta formed atop dendrites expressing Ig2 + 3-GPI ($P = 0.028$) (Figure 7D). Post-synaptic *cis* interactions of the SynCAM 1 Ig2 + 3 domains therefore restrict the size of post- and pre-synaptic specializations.

Discussion

This study analyses the lateral assembly of the synapse-organizing molecule SynCAM 1 and shows that its *cis* interactions organize *trans* adhesion sites. Using live imaging, we find that SynCAM 1 is pre-clustered in neurites prior to synapse assembly. The membrane-proximal Ig2 and Ig3 domains that are not sufficient to form *trans* contacts interact with themselves *in cis* to cluster SynCAM 1 molecules in the

membrane, mediating a self-assembly step that promotes *trans* adhesion. Using the Ig2 + 3 domains in dominant-negative approaches, we provide evidence that they first mediate lateral assembly of SynCAM 1, which in turn promotes clustering at axo-dendritic contacts of young neurons. Later in development, the *cis* oligomerization of SynCAM 1 strengthens its adhesive binding to neuronal partners across the nascent synaptic cleft and supports pre-synaptic induction. Once synapses have formed, the self-assembly of SynCAM 1 within dendritic membranes contributes to restricting the size of synapses.

This study provides mechanistic insight into the steps that assemble SynCAM adhesion sites and highlights the importance of *cis* interactions in organizing Ig protein complexes (Brummendorf and Lemmon, 2001; Aricescu and Jones,
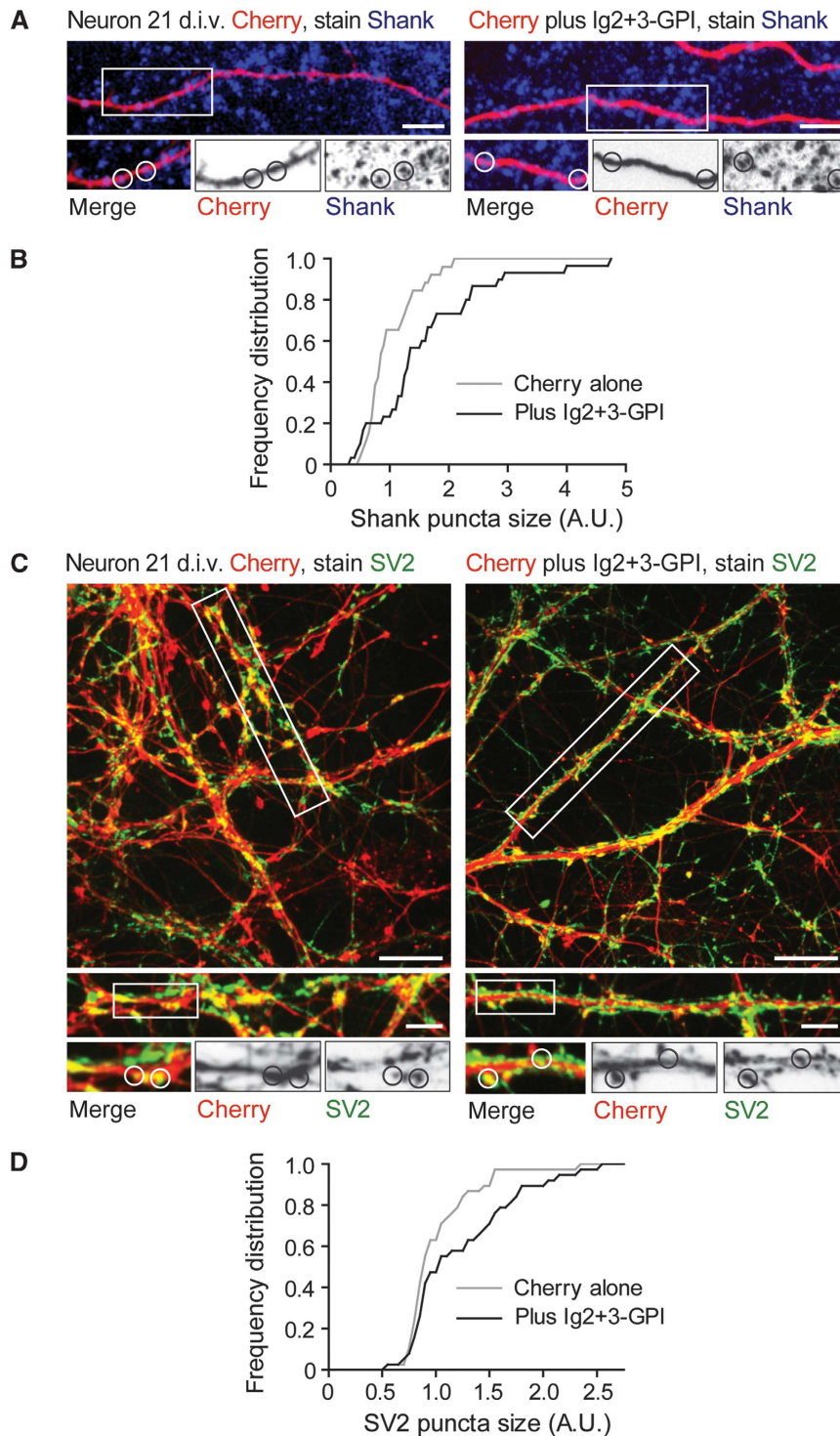
Figure 7 Lateral SynCAM 1 assembly restricts the size of mature synaptic specializations. (**A**) Dissociated hippocampal neurons expressed either Cherry alone (red, left panels) or co-expressed Cherry with GPI-anchored SynCAM 1 Ig2 + 3 (right panels). Neurons were stained at 21 d.i.v. for the excitatory post-synaptic marker Shank (blue). Bottom panels show enlarged dendritic areas, with circles marking dendritic Shank puncta in transfected neurons. Scale bar, 5 μm. (**B**) Cumulative frequency distribution of Shank puncta area imaged as in (**A**). Expression of GPI-anchored SynCAM 1 Ig2 + 3 in dendritic membranes increases the size of post-synaptic specializations ($n = 26$ neurons and 2575 puncta (Cherry alone); 30 neurons and 3271 puncta (Cherry plus Ig2 + 3); three independent experiments). (**C**) Neurons were prepared as in (**A**) and were stained at 21 d.i.v. for the pre-synaptic marker SV2 (green). Top panels show overview images (scale bar, 20 μm), and centre panels depict the dendritic segments marked in the top panels (scale bar, 5 μm). Further enlarged dendritic areas are shown at the bottom, with circles marking SV2 puncta atop transfected neurons. (**D**) Cumulative frequency distribution of SV2 puncta area imaged as in (**C**). Post-synaptic expression of GPI-anchored SynCAM 1 Ig2 + 3 increases the area of pre-synaptic SV2 puncta atop these dendrites ($n = 40$ neurons and 4749 (Cherry alone); 4859 (Cherry plus Ig2 + 3) SV2 puncta; two independent experiments).

2007). Our data indicate that the first extracellular interactions of SynCAM 1 on cell surfaces do not occur with adhesion partners *in trans*, but between SynCAM 1 monomers *in cis*. *Trans* and *cis* interactions are mediated by distinct Ig domains, that is, Ig1 versus Ig2 + Ig3, and can therefore continue once cell–cell adhesion is established. Our findings support the idea that membrane-proximal Ig domains may array extracellular SynCAM sequences into larger complexes, as previously suggested by crystal structures of SynCAM Ig1 domains (Dong *et al*, 2006; Fogel *et al*, 2010). This is reminiscent of the ability of the SynCAM-related nectin proteins to homodimerize *in cis* (Momose *et al*, 2002). Moreover, we show that *cis* dimerization of exogenous SynCAM 1 Ig2 + 3 domains with the full extracellular sequence reduces the latter's capacity to bind *in trans*, possibly by interfering with adhesion-competent orientations of its Ig1 domain. More complete insight into these interactions will require structural studies of the *cis* and *trans* complexes formed by full-length SynCAM extracellular domains, which will extend our molecular understanding of adhesive Ig domain interactions (Freigang *et al*, 2000; Soroka *et al*, 2003; Meijers *et al*, 2007; He *et al*, 2009).

The oligomerization of SynCAM Ig domains in *cis* is of biological relevance as supported by our finding that this lateral self-assembly allows SynCAM 1 to tightly bind its adhesion partners. This result suggests an analogy of SynCAM 1 to the Ig protein L1, where one of its fibronectin type III domains mediates lateral assembly to modulate its Ig domain binding to integrins (Silletti *et al*, 2000). Lateral clustering may promote SynCAM adhesion by increasing the local concentration of binding sites available for *trans* interactions or through sterically positioning the Ig1 domain towards adhesive binding. This could provide a mechanism to initiate and validate synaptic contacts as small *cis* oligomers of SynCAM 1 may grow into large ones as nascent adhesion sites become stable. Similar to SynCAM 1, neuroligin 1 also self-assembles (Dean *et al*, 2003; Gerrow *et al*, 2006) and γ-protocadherins combine into *cis* hetero-multimers (Schreiner and Weiner, 2010). Lateral self-oligomerization may therefore be a property shared by several of the adhesion molecules that organize synaptic membranes. Such a pre-clustering of synaptic membrane proteins into microdomains could be a mechanism to promote signalling once contact between cells occurs, as shown for T-cell receptors (Lillemeier *et al*, 2009). It can now be determined to which extent cell contact may serve as an outside–in signal for SynCAMs to recruit partners such as focal adhesion kinase in promoting synapse assembly (Stagi *et al*, 2010).

Our results also suggest a novel mechanism to regulate SynCAM function by modifying the Ig2 + 3 domains. These modifications may be post-translational to strengthen or weaken binding as shown for the N-glycans at the Ig1 *trans* interface of SynCAM 1 and SynCAM 2 (Fogel *et al*, 2010). In addition, other membrane proteins may compete with SynCAM 1 for binding to its Ig2 + 3 domains, thereby acting as a molecular off-switch for SynCAM lateral assembly and cell adhesion. Interestingly, such heteromeric *cis* interactions of ephrins/EphA receptors and of neurexins/neuroligins have been reported to weaken *trans* interactions (Taniguchi *et al*, 2007; Kao and Kania, 2011), indicating that lateral interactions can provide for the complex regulation of neuronal surface proteins.
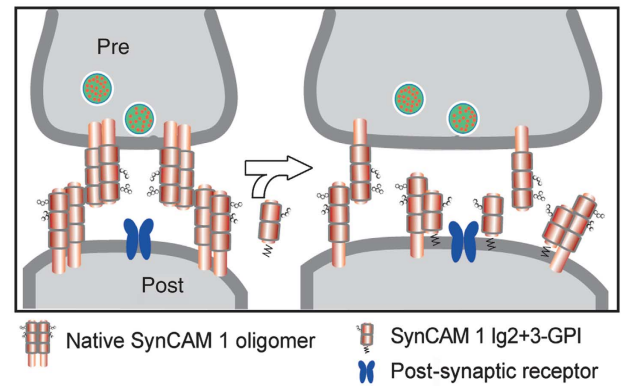

Figure 8 Model of the synaptic roles of lateral SynCAM assembly. Lateral SynCAM interactions strengthen trans-synaptic adhesion and may serve to restrict the size of synaptic specializations (left). Disrupting the underlying Ig2 + 3 *cis* interactions weakens synapse induction and enlarges morphological parameters of synaptic sites (right).

On a macromolecular level, the lateral oligomerization of SynCAMs could contribute to the structural organization of adhesion sites. This would be of particular importance for synapses, which have a structurally well-defined synaptic cleft marked by periodic arrays of protein complexes (Lucic *et al*, 2005; Zuber *et al*, 2005), and also for the structure of myelinated axon junctions (Nans *et al*, 2011), whose formation involves SynCAMs (Maurel *et al*, 2007; Spiegel *et al*, 2007). Considering the prominent expression of SynCAMs in synaptic plasma membranes, where they constitute 0.5% of the total protein (Robbins *et al*, 2010), it is conceivable that SynCAMs may impact structural synaptic properties. This not only agrees with the structural defects of SynCAM 1 knockout mice, which exhibit shortened pre- and post-synaptic membrane specializations (Robbins *et al*, 2010). Such a role of SynCAMs in modulating synapse size is also consistent with our observation that altering the post-synaptic *cis* clustering of SynCAM 1 enlarges post-synaptic specializations and the area occupied by pre-synaptic vesicles. These results support functions of *trans*-synaptic molecules, including SynCAM 1, in modulating synaptic morphological parameters (Figure 8). Such interactions may underlie the high correlation of pre- and post-synaptic structural parameters (Boyer *et al*, 1998). Together, this study identifies the lateral assembly of SynCAM 1 as a molecular feature provided by its two membrane-proximal Ig domains that contributes to the formation and structural organization of synaptic adhesion sites.

Materials and methods

Antibodies
For immunolocalization, antibodies were employed against SynCAM 1 (MBL Laboratories, Nagoya, Japan, CM004-3; 1:1000), SynCAM 1, 2, and 3 proteins (T2412, 1:800; raised in rabbits against the SynCAM 1 carboxyl-terminal sequence that equally recognizes this conserved sequence in SynCAM 2 and 3, but not 4 (Fogel *et al*, 2007)), flag (M2; 1:1000), SV2 (developed by Kathleen Buckley, 1:500; obtained from the Developmental Studies Hybridoma Bank maintained by the University of Iowa), synapsin (Synaptic Systems E028; 1:400), bassoon (Assay Designs VAM-PS003; 1:400), Shank 1–3 (NeuroMab N23B/49; 1:400), PSD-95 (NeuroMab K28/43; 1:400), and MAP2 (Millipore AB364; 1:500). Immunoblotting was performed with mouse monoclonal antibodies against flag (Sigma-Aldrich F1804, clone M2; 1:2000) and the pleio-SynCAM 1/2/3 antibody T2412 (1:2000).

Expression vectors

pCAGGS SynCAM 1-Cherry was generated after PCR amplification of the sequence encoding Cherry from the pRSETB-Cherry vector (a gift from Dr Roger Tsien, University of California, San Diego, CA) as described previously for pCAGGS SynCAM 1-pHluorin (Stagi *et al*, 2010). The SynCAM 1 construct lacking the first Ig domain was obtained after double-digest with *Bmg*BI/*Eco*RV and blunt re-ligation. The pCMV5 flag-GPI vector was generated by amplifying the GPI targeting sequence from GPI-VAMP2 (a gift from Dr James Rothman, Department of Cell Biology, Yale University) with 5′ *Sal*I and 3′ *Bam*HI sites, addition of a 5′ sequence encoding the flag epitope DYKDDDDK, and subcloning into the pCMV5 vector. Sequences encoding full-length SynCAM extracellular sequences or lacking select Ig domains were amplified from pCMV IG9 vectors described previously (Fogel *et al*, 2007) and subcloned into this pCMV5 flag-GPI vector. For neuronal expression of the GPI-tagged Ig2 + 3 construct, the insert was PCR amplified from pCMV5 flag-GPI, cloned into pCR-BluntII-TOPO, and subcloned into pCAGGS using *Eco*RI. GFP was expressed from pCAG GFP, a gift from Dr Nenad Sestan (Yale University, Department of Neurobiology). pCAGGS Cherry was generated after PCR amplification of the sequence encoding Cherry and subcloning using *Eco*RI sites.

Cell culture and protein preparations

COS7 and HEK293 cells were maintained using standard procedures and transfected with FuGENE 6 (Roche Applied Science). Dissociated cultures of hippocampal neurons and mixed co-cultures of COS7 cells were prepared as described (Biederer and Scheiffele, 2007). Expression of the SynCAM extracellular Ig2 + 3 sequence fused to human IgG1-F$_c$ was performed in HEK293 cells as described (Biederer *et al*, 2002) and purified proteins were eluted with glycine pH2.2, adjusted to neutral pH, and dialysed against Modified Tyrode solution (Biederer and Scheiffele, 2007) prior to addition to cultured cells. As negative control, purified human IgG (Sigma, I4506) was adjusted to pH 2.2 and treated in parallel to the purified Ig2 + 3 protein.

Imaging studies

Labelling of SynCAM 1 was performed by addition of specific anti-SynCAM 1 antibodies (MBL Laboratories, CM004-3; 1:400) to live neuronal cultures for 15 min at room temperature in PBS. The neuronal cultures were then washed once and fixed for 15 min with 4% paraformaldehyde in PBS containing 4% sucrose. After fixation, neurons were stained with anti-MAP2 (1:500) and secondary Alexa-dye-conjugated antibodies (Invitrogen; 1:1000). Images were acquired on a Perkin-Elmer UltraView VoX spinning disc microscope equipped with a Hamamatsu C9100-50 camera.

For FRET analysis, COS7 cells were cultured on glass bottom dishes (MatTek, Ashland, MA) and transfected with equal amounts of vectors encoding FRET protein pairs. Cells were imaged 1 day after transfection in Modified Tyrode Solution on a Perkin-Elmer spinning disc microscope equipped with a Hamamatsu C9100-50 camera and a Nikon Perfect Focus autofocus system. Prior to acceptor photobleaching, images were acquired in both green and red channels. A region of interest was then bleached in the red channel using the FRAP unit provided with the spinning disc microscope in membrane areas with strong colocalization between the two transfected proteins. Unless indicated otherwise, we only analysed transfected COS7 cells that were physically isolated from each other to measure FRET within the same cell membrane. Image acquisition was continued, and FRET efficiency was measured as increase in fluorescence intensity in the green channel in the region of interest and quantified by the following standard formula: Fret(EFFICENCY) = {Fdonor(i,j)Bleach−Fdonor(i,j)}/Fdonor(i,j)Bleach, where (i,j) is the position of each pixel. Quantification was performed with a custom-written Matlab (MathWorks) script that is available upon request. FRET efficiencies and statistical information are provided in Supplementary Table S1.

Analyses of SynCAM 1-pHluorin surface expression and growth cone contacts were performed in neurons at 5–6 d.i.v. These neurons were transfected at the time of plating using an Amaxa Nucleofector system (Gaithersburg, MD), following the manufacturer's instructions. Live imaging of dendritic SynCAM 1-pHluorin clusters and measurement of SynCAM 1-pHluorin accumulation at growth cone contacts was performed on a Perkin-Elmer spinning disc microscope as described (Stagi *et al*, 2010). Where indicated, soluble IgG or Ig2 + 3-F$_c$ proteins were added to the live cultured neurons at 100 ng/μl for 2 h at 37 °C, and SynCAM 1-pHluorin cluster density and area were then measured using ImageJ.

Mixed co-culture assays were performed as described (Biederer and Scheiffele, 2007). Briefly, HEK293 cells expressing the proteins of interest and soluble GFP or CFP as transfection marker were plated onto dissociated hippocampal neurons at 8 d.i.v. and fixed and analysed by immunostaining for synaptic markers 2 days later. Where indicated, human IgG or Ig2 + 3-F$_c$ proteins were added at a concentration of 50 ng/μl at the time non-neuronal cells were plated. Images were acquired on a Zeiss LSM 510 confocal microscope and analysed using a custom-written Matlab script that is available upon request.

For studies of marker proteins in mature neurons at 21 d.i.v., cells were transfected at 6–7 d.i.v. with Cherry alone or together with the pCMV5 Ig2 + 3-GPI construct using Lipofectamine LTX and PLUS reagent (Invitrogen). Cells were then fixed and stained as described above. Images were acquired using a Perkin-Elmer spinning disc microscope after averaging image stacks into a single plane. For morphometric analyses, the Cherry signal was used to create a mask identifying dendrites of transfected neurons, and staining parameters of the synaptic markers Shank and SV2 atop those dendrites were measured using a custom-written Matlab script that is available upon request.

Interaction analyses

Cross-linking was performed using COS7 cells at <25% confluency to avoid physical contact of cells, which was visually confirmed prior to reactions. Cells were washed with PBS, treated with BS^3 (Sigma) at 3 mM at room temperature for 30 min, followed by quenching with 50 mM Tris pH 7.0 and lysate collection. SDS–polyacrylamide gel electrophoresis and immunoblotting were performed using standard procedures.

Studies of adhesive interactions by cell overlay assays were performed as described (Thomas *et al*, 2008). Briefly, COS7 cells expressing SynCAM 1 constructs or soluble GFP alone were overlaid with the SynCAM 2 extracellular domain fused to IgG$_1$-F$_c$ (2 μg/ml). Overlaid SynCAM 2 was labelled by including Alexa Fluor 546-Protein A (Invitrogen; 6 μg/ml), while COS7 cell-expressed proteins were detected by adding anti-flag antibodies and secondary Alexa Fluor 488-antibodies (each at 1:1000). Following a 20 min incubation with these detection reagents at room temperature, cells were imaged live on a Nikon Eclipse TE2000-U microscope and signals were quantified using a custom Matlab script that is available upon request.

Data analysis

Statistical analyses were performed using Student's *t*-test and errors correspond to the standard error of mean. All quantitated analyses were performed with the researchers blinded to the conditions.

Supplementary data

Supplementary data are available at *The EMBO Journal* Online (http://www.embojournal.org).

Conflict of interest

The authors declare that they have no conflict of interest.

References

Aricescu AR, Jones EY (2007) Immunoglobulin superfamily cell adhesion molecules: zippers and signals. *Curr Opin Cell Biol* **19:** 543–550

Biederer T (2006) Bioinformatic characterization of the SynCAM family of immunoglobulin-like domain-containing adhesion molecules. *Genomics* **87:** 139–150

Biederer T, Sara Y, Mozhayeva M, Atasoy D, Liu X, Kavalali ET, Südhof TC (2002) SynCAM, a synaptic adhesion molecule that drives synapse assembly. *Science* **297:** 1525–1531

Biederer T, Scheiffele P (2007) Mixed-culture assays for analyzing neuronal synapse formation. *Nat Protoc* **2:** 670–676

Biederer T, Stagi M (2008) Signaling by synaptogenic molecules. *Curr Opin Neurobiol* **18:** 261–269

Boyer C, Schikorski T, Stevens CF (1998) Comparison of hippocampal dendritic spines in culture and in brain. *J Neurosci* **18:** 5294–5300

Brummendorf T, Lemmon V (2001) Immunoglobulin superfamily receptors: cis-interactions, intracellular adapters and alternative splicing regulate adhesion. *Curr Opin Cell Biol* **13:** 611–618

Dean C, Scholl FG, Choih J, DeMaria S, Berger J, Isacoff E, Scheiffele P (2003) Neurexin mediates the assembly of presynaptic terminals. *Nat Neurosci* **6:** 708–716

Dong X, Xu F, Gong Y, Gao J, Lin P, Chen T, Peng Y, Qiang B, Yuan J, Peng X, Rao Z (2006) Crystal structure of the V domain of human Nectin-like molecule-1/Syncam3/Tsll1/Igsf4b, a neural tissue-specific immunoglobulin-like cell-cell adhesion molecule. *J Biol Chem* **281:** 10610–10617

Fogel AI, Akins MR, Krupp AJ, Stagi M, Stein V, Biederer T (2007) SynCAMs organize synapses through heterophilic adhesion. *J Neurosci* **27:** 12516–12530

Fogel AI, Li Y, Giza J, Wang Q, Lam TT, Modis Y, Biederer T (2010) N-glycosylation at the SynCAM (synaptic cell adhesion molecule) immunoglobulin interface modulates synaptic adhesion. *J Biol Chem* **285:** 34864–34874

Freigang J, Proba K, Leder L, Diederichs K, Sonderegger P, Welte W (2000) The crystal structure of the ligand binding module of axonin-1/TAG-1 suggests a zipper mechanism for neural cell adhesion. *Cell* **101:** 425–433

Gerrow K, Romorini S, Nabi SM, Colicos MA, Sala C, El-Husseini A (2006) A preformed complex of postsynaptic proteins is involved in excitatory synapse development. *Neuron* **49:** 547–562

Giagtzoglou N, Ly CV, Bellen HJ (2009) Cell adhesion, the backbone of the synapse: 'vertebrate' and 'invertebrate' perspectives. *Cold Spring Harb Perspect Biol* **1:** a003079

Gray EG (1959) Axo-somatic and axo-dendritic synapses of the cerebral cortex: an electron microscope study. *J Anat* **93:** 420–433

Harrison OJ, Bahna F, Katsamba PS, Jin X, Brasch J, Vendome J, Ahlsen G, Carroll KJ, Price SR, Honig B, Shapiro L (2010) Two-step adhesive binding by classical cadherins. *Nat Struct Mol Biol* **17:** 348–357

He Y, Jensen GJ, Bjorkman PJ (2009) Cryo-electron tomography of homophilic adhesion mediated by the neural cell adhesion molecule L1. *Structure* **17:** 460–471

Jin Y, Garner CC (2008) Molecular mechanisms of presynaptic differentiation. *Annu Rev Cell Dev Biol* **24:** 237–262

Kao T-J, Kania A (2011) Ephrin-mediated cis-attenuation of Eph receptor signaling is essential for spinal motor axon guidance. *Neuron* **71:** 76–91

Kwiatkowski AV, Weis WI, Nelson WJ (2007) Catenins: playing both sides of the synapse. *Curr Opin Cell Biol* **19:** 551–556

Lillemeier BF, Mortelmaier MA, Forstner MB, Huppa JB, Groves JT, Davis MM (2009) TCR and Lat are expressed on separate protein islands on T cell membranes and concatenate during activation. *Nat Immunol* **11:** 90–96

Lucic V, Yang T, Schweikert G, Forster F, Baumeister W (2005) Morphological characterization of molecular complexes present in the synaptic cleft. *Structure* **13:** 423–434

Masuda M, Yageta M, Fukuhara H, Kuramochi M, Maruyama T, Nomoto A, Murakami Y (2002) The tumor suppressor protein TSLC1 is involved in cell-cell adhesion. *J Biol Chem* **277:** 31014–31019

Maurel P, Einheber S, Galinska J, Thaker P, Lam I, Rubin MB, Scherer SS, Murakami Y, Gutmann DH, Salzer JL (2007) Nectin-like proteins mediate axon Schwann cell interactions along the internode and are essential for myelination. *J Cell Biol* **178:** 861–874

Meijers R, Puettmann-Holgado R, Skiniotis G, Liu JH, Walz T, Wang JH, Schmucker D (2007) Structural basis of Dscam isoform specificity. *Nature* **449:** 487–491

Momose Y, Honda T, Inagaki M, Shimizu K, Irie K, Nakanishi H, Takai Y (2002) Role of the second immunoglobulin-like loop of nectin in cell-cell adhesion. *Biochem Biophys Res Commun* **293:** 45–49

Nam CI, Chen L (2005) Postsynaptic assembly induced by neurexin-neuroligin interaction and neurotransmitter. *Proc Natl Acad Sci USA* **102:** 6137–6142

Nans A, Einheber S, Salzer JL, Stokes DL (2011) Electron tomography of paranodal septate-like junctions and the associated axonal and glial cytoskeletons in the central nervous system. *J Neurosci Res* **89:** 310–319

Robbins EM, Krupp AJ, Perez de Arce K, Ghosh AK, Fogel AI, Boucard A, Sudhof TC, Stein V, Biederer T (2010) SynCAM 1 adhesion dynamically regulates synapse number and impacts plasticity and learning. *Neuron* **68:** 894–906

Rostaing P, Real E, Siksou L, Lechaire JP, Boudier T, Boeckers TM, Gertler F, Gundelfinger ED, Triller A, Marty S (2006) Analysis of synaptic ultrastructure without fixative using high-pressure freezing and tomography. *Eur J Neurosci* **24:** 3463–3474

Schikorski T, Stevens CF (1997) Quantitative ultrastructural analysis of hippocampal excitatory synapses. *J Neurosci* **17:** 5858–5867

Schreiner D, Weiner JA (2010) Combinatorial homophilic interaction between gamma-protocadherin multimers greatly expands the molecular diversity of cell adhesion. *Proc Natl Acad Sci USA* **107:** 14893–14898

Silletti S, Mei F, Sheppard D, Montgomery AM (2000) Plasmin-sensitive dibasic sequences in the third fibronectin-like domain of L1-cell adhesion molecule (CAM) facilitate homomultimerization and concomitant integrin recruitment. *J Cell Biol* **149:** 1485–1502

Sivasankar S, Zhang Y, Nelson WJ, Chu S (2009) Characterizing the initial encounter complex in cadherin adhesion. *Structure* **17:** 1075–1081

Soroka V, Kolkova K, Kastrup JS, Diederichs K, Breed J, Kiselyov VV, Poulsen FM, Larsen IK, Welte W, Berezin V, Bock E, Kasper C (2003) Structure and interactions of NCAM Ig1-2-3 suggest a novel zipper mechanism for homophilic adhesion. *Structure* **11:** 1291–1301

Spiegel I, Adamsky K, Eshed Y, Milo R, Sabanay H, Sarig-Nadir O, Horresh I, Scherer SS, Rasband MN, Peles E (2007) A central role for Necl4 (SynCAM4) in Schwann cell-axon interaction and myelination. *Nat Neurosci* **10:** 861–869

Stagi M, Fogel AI, Biederer T (2010) SynCAM 1 participates in axo-dendritic contact assembly and shapes neuronal growth cones. *Proc Natl Acad Sci USA* **107:** 7568–7573

Takeichi M (2007) The cadherin superfamily in neuronal connections and interactions. *Nat Rev Neurosci* **8:** 11–20

Taniguchi H, Gollan L, Scholl FG, Mahadomrongkul V, Dobler E, Limthong N, Peck M, Aoki C, Scheiffele P (2007) Silencing of neuroligin function by postsynaptic neurexins. *J Neurosci* **27:** 2815–2824

Thomas LA, Akins MR, Biederer T (2008) Expression and adhesion profiles of SynCAM molecules indicate distinct neuronal functions. *J Comp Neurol* **510:** 47–67

Troyanovsky RB, Laur O, Troyanovsky SM (2007) Stable and unstable cadherin dimers: mechanisms of formation and roles in cell adhesion. *Mol Biol Cell* **18:** 4343–4352

Wouters FS, Verveer PJ, Bastiaens PI (2001) Imaging biochemistry inside cells. *Trends Cell Biol* **11:** 203–211

Zhang Y, Sivasankar S, Nelson WJ, Chu S (2009) Resolving cadherin interactions and binding cooperativity at the single-molecule level. *Proc Natl Acad Sci USA* **106:** 109–114

Zuber B, Nikonenko I, Klauser P, Muller D, Dubochet J (2005) The mammalian central nervous synaptic cleft contains a high density of periodically organized complexes. *Proc Natl Acad Sci USA* **102:** 19192–19197

SUPPLEMENTAL DATA

LATERAL ASSEMBLY OF THE IMMUNOGLOBULIN PROTEIN SYNCAM 1 CONTROLS ITS ADHESIVE FUNCTION AND INSTRUCTS SYNAPSE FORMATION

Adam I. Fogel [1,2]✤, Massimiliano Stagi [1,3]✤, Karen Perez de Arce [1]✤, and Thomas Biederer [1]*

[1] Department of Molecular Biophysics and Biochemistry, Yale University, New Haven, CT 06520

[2] current address: National Institute of Neurological Disorders and Stroke, NIH, Bethesda, MD 20892

[3] current address: Department of Neurology, Yale University, New Haven, CT 06520

✤ these authors contributed equally to this study

SUPPLEMENTAL FIGURE LEGENDS

Supplemental Figure 1. Lack of FRET in live negative control cells.

A. Soluble Cherry and GFP were co-expressed in COS7 cells and FRET was analyzed by acceptor photobleaching as in Figure 2 of the main text. Top row, Cherry signal (left column) and its merged image with the GFP signal (right) before photobleaching of Cherry. Bottom, fluorescence signals immediately after bleaching of the boxed area.

B. No FRET signal was measured in A. The fraction of pixels for which FRET was measured after photobleaching was with $0.26 \pm 0.21\%$ at background level (n=4 cells).

Supplemental Figure 2. Membrane-proximal regions of SynCAM 1 are not closely apposed at *trans* adhesion sites.

A. No FRET occurred between SynCAM 1-pHluorin and SynCAM 1-Cherry when expressed separately in COS7 cells contacting each other. FRET was analyzed by acceptor photobleaching of cell contact areas. Top row, Cherry signal (left column) and its merged image with the pHluorin signal (right) before photobleaching. Bottom, the same channels immediately after bleaching of the marked area.

B. No FRET signal was measured in A. The fraction of pixels in which FRET was measured after photobleaching was with $5.9 \pm 3.6\%$ at background levels (n=4 cells).

C. Model of the pHluorin and Cherry-tagged SynCAM 1 FRET pairs expressed in separate cells. The lack of FRET is consistent with SynCAM adhesion pairs extending into a conformation that separates their membrane-proximal regions beyond the distance of 10 nm detectable by FRET.

Supplemental Figure 3. Control of GPI-anchored SynCAM 1 construct expression.

A. Surface expression of SynCAM 1 ECD ^{flag} GPI was not affected by co-expression of GPI-anchored Ig2+3. Surface expressed ECD ^{flag} GPI protein was detected in live COS7 cells by overlay with anti-flag antibodies and secondary fluorescent antibodies as in Figure 4A of the main text.

B. Immunoblot analysis of the lysates analyzed in A. with antibodies against SynCAM 1 showed that co-expression of GPI-anchored Ig2+3 did not alter the total amounts of SynCAM 1 ECD ^{flag} GPI. Co-expressed GFP served as loading control.
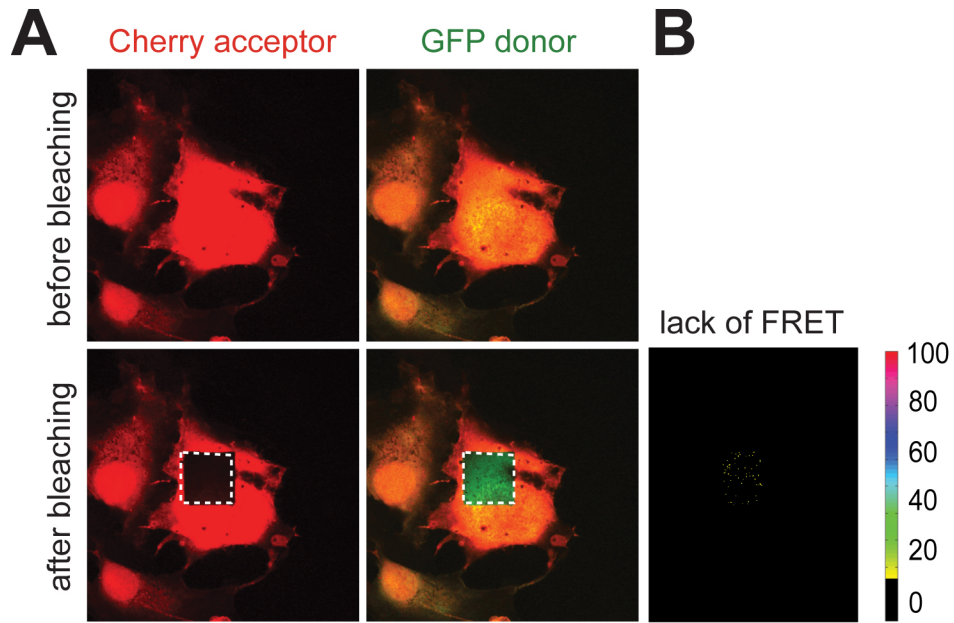
Supplemental Figure 4. Localization of GPI-anchored SynCAM 1 in neurons.

A. Flag-tagged SynCAM 1 Ig2+3-GPI was expressed in rat hippocampal neurons and analyzed at 21 d.i.v. by immunostaining for flag (red), the presynaptic marker synapsin (green), and the postsynaptic marker PSD-95 (blue). The boxed area is enlarged in B. Scale bar, 10 μm.
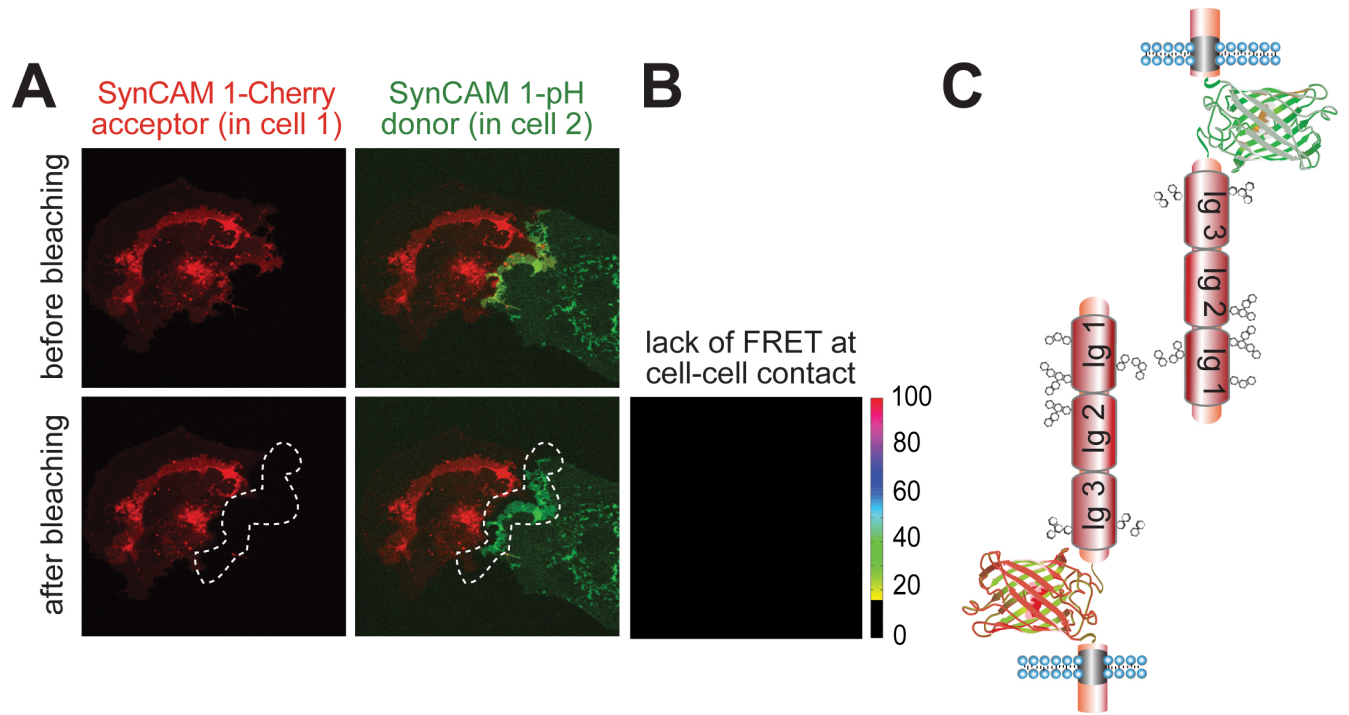
B. Top panel, enlarged image of the boxed area in A. Bottom panels show the channels individually. Ig2+3 ^{flag}-GPI formed clusters when expressed in neurons. Smaller clusters predominantly co-localized with the synaptic markers synapsin and PSD-95 and a subset is marked with circles. Larger clusters presumably correspond to aggregates of Ig2+3 ^{flag}-GPI formed by lateral self-assembly. Scale bar, 10 μm.

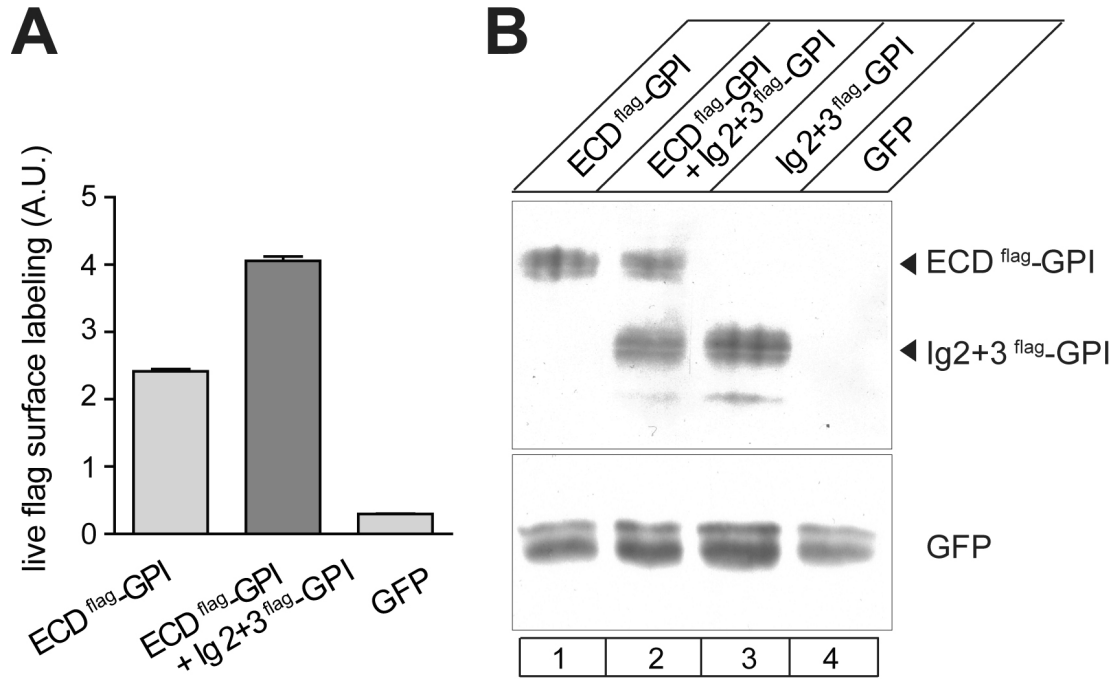**Supplemental Table 1. Quantification of FRET data.**

For each experiment, n=4-6 cells were analyzed. % pixel FRET is the percentage of pixels within the photobleached area that exhibited FRET. A 15% value in the FRET matrix was chosen as cut-off for FRET detection. FRET efficiency is the average efficiency of FRET observed for pixels in the photobleached area. The mean and standard deviation for each of these parameters are shown.

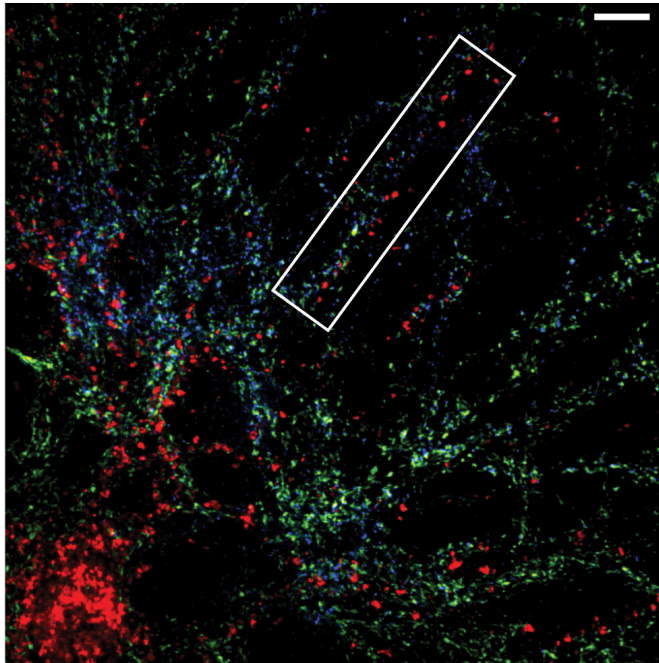**Supplemental Figure 1**

A SynCAM 1-Cherry acceptor (in cell 1) SynCAM 1-pH donor (in cell 2)

before bleaching

after bleaching

B lack of FRET at cell-cell contact

C

Supplemental Figure 2

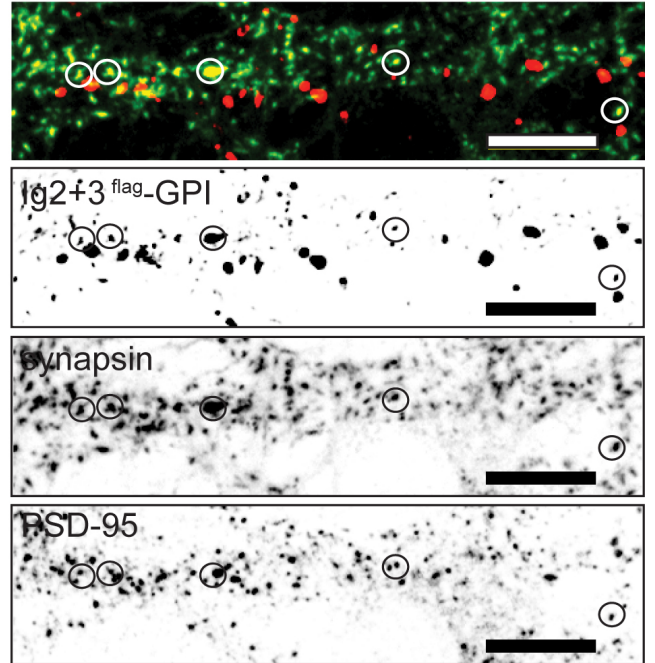**A**

B

Supplemental Figure 3

A

neurons 21 d.i.v. expression Ig2+3 flag-GPI
stain flag / synapsin / PSD-95

B

Ig2+3 flag-GPI / synapsin

Supplemental Figure 4

Conditions	Sample Number	% Pixel FRET	FRET Efficiency in Pixels with FRET	Standard Deviation of FRET Efficiency
SynCAM 1pH CIS SynCAM 1Ch	1	44.25	30.24	10.22
SynCAM 1pH CIS SynCAM 1Ch	2	23.48	29.59	9.73
SynCAM 1pH CIS SynCAM 1Ch	3	15.56	32.67	9.79
SynCAM 1pH CIS SynCAM 1Ch	4	28.64	28.56	9.8
SynCAM 1pH CIS SynCAM 1Ch	5	27.8	28.43	10.4
SynCAM 1pH CIS SynCAM 1Ch	6	36	29.98	10.16
	average	29.29	29.91	10.02
	standard deviation	9.94	1.54	0.28
SynCAM 1pH CIS SynCAM 1 Ig2+3Ch	1	4.48	24.34	7.43
SynCAM 1pH CIS SynCAM 1 Ig2+3Ch	2	16.04	25.59	7.80
SynCAM 1pH CIS SynCAM 1 Ig2+3Ch	3	12.31	34.00	11.42
SynCAM 1pH CIS SynCAM 1 Ig2+3Ch	4	17.43	35.88	11.15
SynCAM 1pH CIS SynCAM 1 Ig2+3Ch	5	19.53	31.48	9.26
	average	13.96	30.26	9.41
	standard deviation	5.92	5.10	1.84
SynCAM 1pH TRANS SynCAM 1Ch	1	6.31	31.35	20.08
SynCAM 1pH TRANS SynCAM 1Ch	2	6.38	27.02	11.52
SynCAM 1pH TRANS SynCAM 1Ch	3	9.85	27.45	15.38
SynCAM 1pH TRANS SynCAM 1Ch	4	1.04	22.18	5.1
	average	5.90	27.00	13.02
	standard deviation	3.63	3.76	6.33
GFP soluble PLUS Cherry soluble	1	0.18	26.09	0.9
GFP soluble PLUS Cherry soluble	2	0.56	26.11	0.9
GFP soluble PLUS Cherry soluble	3	0.19	34.25	21.28
GFP soluble PLUS Cherry soluble	4	0.09	28.64	11.97
	average	0.26	28.77	8.76
	standard deviation	0.21	3.84	9.84

Supplemental Table 1